

# Microstructural characterization of glass fiber reinforced SMC by nanoindentation and single-fiber push-out test

B. Rohrmüller<sup>1,2</sup>, P. Gumbsch<sup>1,2</sup>, J. Hohe<sup>1</sup>,

<sup>1</sup>Fraunhofer-Institute for Mechanics of Materials IWM, Wöhlerstraße 11, 79108 Freiburg, Germany,

<sup>2</sup>Karlsruhe Institute of Technology (KIT), Institute for Applied Materials, Kaiserstr. 12, 76131 Karlsruhe, Germany

## 1 Introduction

Fiber reinforced polymers (FRPs) are due to their high strength and low density an important material group in lightweight constructions. Due to their low density in comparison to metals they help to reduce weight and like this reduce fuel consumption in the mobility sector.

The investigated material is glass fiber reinforced Sheet-Molding-Compound (SMC), which has due to its production process a bundle microstructure [8]. The polymer is unsaturated polyesther polyurethan hybrid (UPPH), a thermoset.

When we look on the microstructural level, FRPs are characterized by the behavior of fibers, matrix and the connecting fiber-matrix interface. That means that beneath the properties of fibers and matrix material, the interface also has a substantial contribution to the overall performance of a composite, as can be found for example in [3].

The aim of this contribution is to characterize numerically the fiber-matrix interface by FEM-simulations. This is done by experimental and numerical single-fiber push-out tests. In literature push-out tests are often simulated with an isotropic linear elastic matrix material model [1],[3]. In [6] push-out tests were simulated with an elasto-plastic matrix material model, which led to a better agreement instead of only using a linear elastic matrix material model.

Here we use a nonlinear elastic hyperelastic material model with a Prony series for viscoelasticity to describe the UPPH matrix. The UPPH matrix is characterized by nanoindentation tests on matrix rich regions of the composite, followed by FEM-simulations to calibrate the model. In a second step the calibrated matrix model, as well as from cyclic single-fiber push-out tests experimentally determined fracture toughness is used as input for a push-out simulation model. The interface strength is adapted to get an agreement between simulation and experimental push-out tests.

## 2 Methods

Nanoindentation tests are done on matrix rich regions of the composite to characterize the matrix behavior. Afterwards a simulation model of the indentation is built up to adjust the parameters of a hyperelastic material law with viscoelastic effects to describe the matrix. A Neo-Hooke model with a Prony series for viscoelasticity is used therefore.

Single-fiber push-out tests are conducted to characterize the debonding between fiber and matrix.

In a single-fiber push-out test a single fiber, laying vertically in a thin polished specimen, is loaded by a indenter tip to get a force displacement curve of the debonding. The single-fiber push-out tests are conducted quasi-statically and cyclic. The motivation for the cyclic single-fiber push-out tests is to determine experimentally the fracture toughness of the debonding between fiber and surrounding

matrix material. The method was proposed by [9] for ceramic composites and further developed for fiber reinforced polymers by [6],[7]. The experimentally determined fracture toughness is then used in the modelling of the interface for the push-out simulation.

## 2.1 Experiment

For the described nanoindentation and push-out experiments was used a TI-950 TriboIndenter from Hysitron.

### 2.1.1 Nanoindentation test

The nanoindentation tests in matrix rich regions from the composite were done with a diamond Berkovich modified tip, a three-sided pyramid with a half angle of  $65.27^\circ$ . The material specimens were cut out of the cross section of a material plate and polished on the surface. The polished specimens with a thickness of 1 mm were glued on a sample holder for testing. For the loading curve the loading rate divided by the load  $\dot{P}/P$  is held constant. The loading curve is followed by a hold time with constant force for 100 s during which the displacement is increasing due to viscoelasticity. An exemplary curve with  $\dot{P}/P = 2/s$  can be seen in Figure 4 (left).

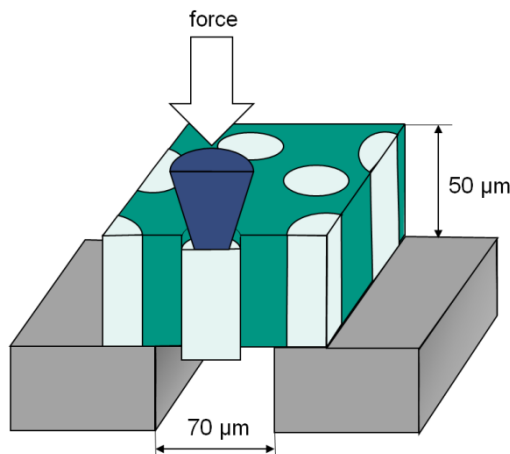


**Figure 1:** Sketch of single-fiber push-out test.

### 2.1.1 Single-fiber push-out test

For the specimen preparation of the push-out test slices with a thickness of 1mm were cut from the cross section of a material plate. The slices of material were ground and polished on both sides. The thickness of the specimens at the end of the polishing process was at about  $50\ \mu\text{m}$ . The tested fibers are perpendicular to the surface and lay during the testing over a groove with a thickness of  $70\ \mu\text{m}$  as can be seen in Figure 1. The specimen is glued on the sample holder during testing to reduce the compliance of the system. The indenter tip is a conical flat end indenter tip out of diamond with a diameter of  $5\ \mu\text{m}$  and an angle of  $60^\circ$ . As the diameter of the glass fibers is at about  $13\ \mu\text{m}$ , the indenter tip only touches the fiber during the testing and not the surrounding matrix material. The tests are conducted displacement controlled with a displacement rate of  $50\ \text{nm/s}$ .

The tests are done quasi-static with increasing displacement until  $5\ \mu\text{m}$  and cyclic with loading and unloading cycles with increments of  $200\ \text{nm}$  per cycle, also until  $5\ \mu\text{m}$ . An exemplary resulting force displacement curve for a cyclic push-out test can be seen in Figure 2. The middle and right picture shows the corresponding fiber after the test from front and backside.

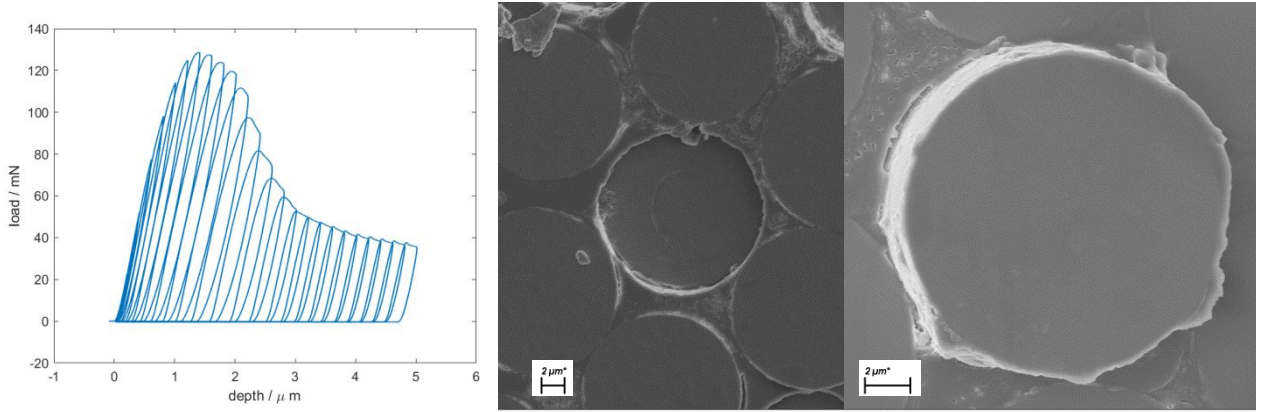


**Figure 2:** load-displacement curve of cyclic push-out test (left), pushed-in fiber on front surface (middle) and push-out fiber on the backside (right).

It can be observed a successive push-out behavior, as also observed in the literature in [7] for carbon fiber reinforced polyether ether ketone. That means we have a stable crack growth from the push-in of the fiber in the matrix on the front side until the push-out on the back side at a displacement of 3  $\mu\text{m}$ . The nearly constant level of maximum force after a displacement of 3  $\mu\text{m}$  is induced by friction between the debonded fiber from the surrounding matrix.

The cyclic push-out tests are evaluated energetically by separating each loading and unloading cycle in its elastic, friction and fracture energy contribution as proposed by [9],[6],[7].

## 2.2 Simulation

The matrix material and the fiber-matrix interface are characterized by FEM simulations.

### 2.2.1 Nanoindentation simulations

To determine more parameters than modulus and hardness, as classically done in nanoindentation testing, it is necessary to simulate the experiment in order to fit the simulation curve to the experiment by adapting the model parameters as for example done by [1].

The matrix material is simulated by the hyperelastic Neo-Hooke model with a Prony series for viscoelasticity. The strain energy potential for the Neo-Hooke model is given by

$$U = C_{10}(\bar{I}_1 - 3) + \frac{1}{D_1} (J - 1)^2 \quad (1)$$

with the deviatoric strain invariant  $\bar{I}_1$ , the determinant of the deformation gradient  $J$  and the material parameters  $C_{10}$  and  $D_1$ . The first part of the potential is incompressible and the second part compressible. More information on hyperelastic material models can for example be found in [5]. The parameters  $C_{10}$  and  $D_1$  become time dependent to add viscoelastic behavior to the model. Therefore a Prony series is introduced for the dimensionless shear and compression modulus

$$g_R(t) = 1 - \sum_{i=1}^N \bar{g}_i^P (1 - e^{-t/\tau_i}) \quad (2)$$

$$k_R(t) = 1 - \sum_{i=1}^N \bar{k}_i^P (1 - e^{-t/\tau_i}) \quad (3)$$

with the material parameters  $\bar{g}_i^P$ ,  $\bar{k}_i^P$  and  $\tau_i$  and the number of series parameters  $N$ . The parameters of the Neo-Hooke model can then be written as

$$C_{10}(t) = \frac{C_{10}^\infty}{1 - \sum_{i=1}^N \bar{g}_i^P} g_R(t), \quad (4)$$

$$D_1(t) = \frac{D_1^\infty}{k_R(t)} \left(1 - \sum_{i=1}^N \bar{k}_i^P\right). \quad (5)$$

The parameters  $C_{10}^\infty$  and  $D_1^\infty$  are describing the equilibrium curve after complete relaxation. For the simulation model a 60° 3D model of experiment is rebuilt as for example done in [4]. As for the simulation of the quasi-static push-out tests only loading and not unloading is considered, the simulation model of the nanoindentation is fitted only to the loading and holding part of the curve.

### 2.2.2 Single-fiber push-out test simulation

Simulations of the quasi-static push-out test are done to investigate the interface behavior and to determine interface model parameters. The simulation model can be seen in Figure 3. The indented fiber is surrounded by matrix material in which are embedded other fibers. The matrix is embedded in composite material. The diamond indenter tip is modelled as a rigid body, as diamond has a very high stiffness in comparison to glass fibers. The glass fibers are modelled as isotropic linear elastic with a Young's modulus of 73 GPa and a Poisson's ratio of 0.22. The matrix model and parameters are taken from the nanoindentation simulation. The fiber-matrix interface is modelled by cohesive

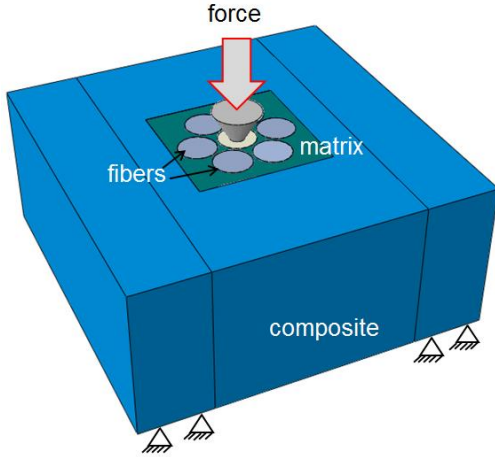


**Figure 3:** simulation model of single-fiber push-out test.

zone contacts with an uncoupled traction separation law. A quadratic stress criterion is used for damage initiation. The damage evolution is described by a power law form and linear softening. The parameters to adjust are the stiffness, the fracture toughness and the interface strength. The stiffness is a numerical value, the fracture toughness is determined from cyclic push-out tests and the strength is finally adapted on the quasi-static experimental push-out curves.

## 3 Results

The experimental nanoindentation force displacement curve with the fitted simulation curve for the loading and holding part is depicted in Figure 4 on the left. The resulting matrix model parameters are given in Table 1.

**Table 1.** Matrix material model parameters.

$C_{10}^\infty$	$D_1^\infty$	$i$	$\bar{g}_i^P$	$\bar{k}_i^P$	$\tau_i$ in s
724 MPa	0.01 1/MPa	1	0.13	0.11	2.9
		2	0.04	0.17	10
		3	0.009	0.22	720

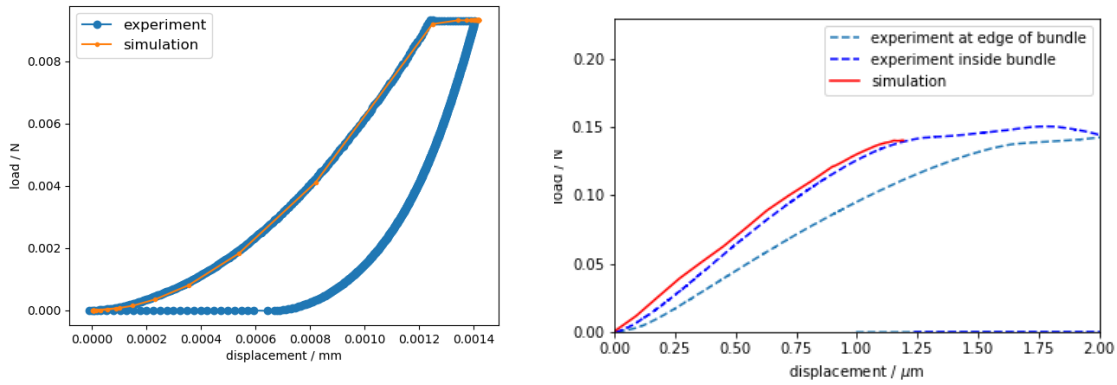


**Figure 4:** experimental and simulation results of nanoindentation (left) and push-out test (right).

The resulting fracture toughness from the cyclic push-out tests for 13 tested fibers is  $107 \pm 20 \text{ J/m}^2$ . For the push-out simulations a fracture toughness value for the interface of  $107 \text{ J/m}^2$  is used. In Figure 4 (right) can be seen the experimental and simulation results for the push-out test. The simulation model, which models a fiber inside a bundle, can be adjusted with an interface strength of 70 MPa in normal and shear directions to the experimental curve of a fiber inside a bundle. The experimental curve of a fiber at the edge of a bundle shows a lower slope.

The slight shift between experiment and simulation can be explained by the fact that the surfaces in

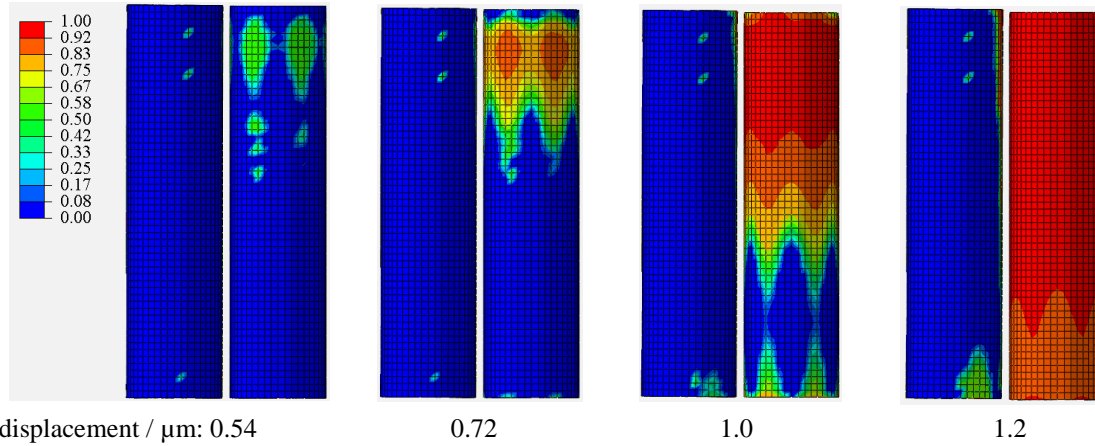


**Figure 5:** Interface damage evolution (0 undamaged, 1 completely damaged) for different displacements, indented fiber always on the right side, only one neighboring fiber is shown.

the simulation model between indenter tip and fiber are completely flat, while the fiber surface in experiment is slightly concave and there is no complete contact at the beginning of the test. The interface degradation for increasing displacements is shown in Figure 5. It can be seen a higher interface degradation where fibers are close together. The interface is not only damaged at the pushed-out fiber but also at the neighboring fibers.

## 4 Conclusion

The single-fiber push-out test could be investigated in experiment and simulation with an hyperelastic viscous matrix material model. The matrix model is calibrated on nanoindentation experiments with FEM-simulations. The push-out simulation model can be adapted to get a good agreement between experiment and simulation until the maximum force, even if there is a small shift in displacement because the concave fiber surface in experiment is not modelled. What cannot be modelled is the successive push-out behavior after the maximum force. In the simulation the interface is nearly destroyed at the maximum force. What might be added to simulation are production induced residual stresses due to temperature cooling and curing which are present in experiment.

## 5 Acknowledgement

The research documented in this manuscript has been funded by the German Research Foundation (DFG) within the International Research Training Group “Integrated engineering of continuous-discontinuous long fiber-reinforced polymer structures” (GRK 2078). The support by the German Research Foundation (DFG) is gratefully acknowledged. The support of David Bücheler and Sergej Ilinzeer (Fraunhofer Institute for Chemical Technology) for the UPPH SMC based composite production is appreciated.

## 6 References

- [1] B. Brylka, F. Fritzen, T. Böhlke, K.A. Weidenmann, *Proc. Appl. Math. Mech.* 11, 141 – 142 **2011**.
- [2] Z. Chen, S. Diebels, *Technische Mechanik*, 34, 3-4, **2014**, p. 166 – 189.
- [3] S. Fliegenger, *Micromechanical finite element modeling of long fiber reinforced thermoplastics*, Fraunhofer Verlag, Stuttgart, **2016**.
- [4] M. Hardiman, *Nanoindentation characterisation of carbon fibre reinforced plastic microstructures*, University of Limerick, **2016**.
- [5] G. A. Holzapfel, *Nonlinear Solid Mechanics: a continuum approach for engineering*, John Wiley & Sons, Chichester, **2000**.
- [6] J. Jäger, M.G.R. Sause, F. Burkert, J. Moosburger-Will, M. Greisel, S. Horn, *Composites: Part A* 71, **2015**, p. 157–167.
- [7] J. Moosburger-Will, M. Greisel, M. Schulz, M. Löffler, W.M. Mueller, S. Horn, *Composite Interfaces*, **2019**.
- [8] P. Pinter, *Microstructure characterization of continuous-discontinuous fibre reinforced polymers based on volumetric images*, KIT Scientific Publishing, Karlsruhe, **2018**, p. 42.
- [9] W.M. Mueller, J. Moosburger-Will, M.G.R. Sause, S. Horn, *Journal of the European Ceramic Society* 33, **2013**, p. 441–451.